

A neutron shielding Monte Carlo study for the Coherent Elastic Neutrino Nucleus Scattering experiment

A. Olivier

*Louisiana State University, Baton Rouge, LA 70803
Fermi National Accelerator Laboratory, Batavia, IL 60510*

The development and results of a Monte Carlo study for an off-axis neutron shielding experiment for the Coherent Elastic Neutrino Nucleus Scattering (CENNS) experiment at the Fermi National Accelerator Laboratory Booster Neutrino Beamline (BNB) are presented. The spectra of neutrons that pass through several configurations of concrete shielding blocks are considered, and a shielding geometry is identified that yields the smallest number of expected events in the 10-30 MeV range where neutron interactions with nuclei are expected to be a dangerous background to CENNS experiments. The expected reduction in neutron flux inside the best shielding geometry is given, and the effect of shielding thickness on neutron spectrum attenuation is presented. Further problems with shielding strategies to be considered using this Monte Carlo simulation are stated.

I. INTRODUCTION

With much of high-energy particle physics focused on searches for rare processes such as neutrino and dark matter interactions with nuclei, experimental results for Standard Model predictions of coherent elastic neutrino-nucleus scattering have great potential to contribute to future Intensity Frontier experiments. The Coherent Elastic Neutrino Nucleus Scattering or CENNS experiment is a liquid argon detector designed to search for this rare process by detecting nuclear recoil in Argon atoms. Since low-energy neutrinos best fulfill the condition of coherence, the CENNS detector will be placed far off axis at the Fermi National Accelerator Laboratory Booster Neutrino Beamline (BNB) outside the beam target building. Observation of CENNS could have implications for sterile neutrino searches and backgrounds in dark matter direct detection experiments, and significant deviation of the cross section for this process from the Standard Model prediction could reveal hints of new physics. Therefore, results of the CENNS experiment will likely have relevance to a broad range of questions in high-energy physics.

While developments in technology for searching for rare processes have made the level of precision necessary for the CENNS detector achievable, low-energy neutrons produced near the BNB target can cause nuclear recoil in the detector very similar to the effects of neutrino scattering. In addition, any shielding introduced to reduce the low energy neutron background for the CENNS detector may produce more low-energy neutrons. Thus, a study using the SciBath detector to evaluate the effectiveness of various arrangements of concrete shielding blocks in decreasing the flux of low-energy neutrons has been proposed to better understand this large contribution to the background for the CENNS experiment. A Monte Carlo study has been developed to predict the effectiveness of various shielding strategies in attenuating the spectrum of low energy neutrons from the BNB. These predictions will be compared to experimental results from the SciBath detector and used to develop a more effective Monte Carlo simulation to design shielding for the CENNS experiment.

To understand the neutron background near the BNB target, the SciBath detector was used to observe the neutron flux in the BNB target building. A detailed treatment of this study and its results is provided in Reference¹. The neutron flux recorded by SciBath in 2012 was used to create a rough flux file for input to this Monte Carlo study.

II. METHODS

The G4Beamline² simulation package was chosen for the Monte Carlo study of neutron shielding for CENNS because of the reliability of the physics package on which it is based, Geant4, its relatively simple interface to the Geant4 geometry system, and its ability to take plain text beam files as input and produce ROOT files as output. The beam file was required by G4Beamline to be in the BLTrackFile format, so a script was written to produce a distribution of neutrons based on the neutron kinetic energy spectrum measured in the work described in Reference¹.

CERN's ROOT analysis framework was used for the generator script to take advantage of the random number generators and physics data objects it provides. In the generator script, kinetic energy bins are created based on the data presented in Figure 14 of Reference¹. Bin sizes are determined based on user input for the number of particles to be generated. The implementation of the Mersenne Twister pseudo-random number generator in ROOT Version 5.34 is used to produce random positions and momenta. In later versions of the script, the user specifies whether the particles generated will have momenta along or at $\pm 45^\circ$ relative to the beam axis. To produce the correct distribution of momenta, enough random momentum values to fill each kinetic energy bin are multiplied by the difference between the lower edge of the bin they are selected for and the next highest bin. Then, the lower edge of each bin is added to the momentum values that bin contains. Since this places the momenta in increasing order, an array containing the random momenta is shuffled using a custom random shuffle function. At the end of the generator script, the neutron parameters produced are written to an ASCII file in the BLTrackFile format documented in Reference².

Once suitable beam files are produced, G4Beamline configuration files are used to implement detector and shielding geometries and control simulations. G4Beamline uses a simplified form of the syntax of Geant4 to construct geometries using Geant methods. All basic geometries are constructed using boxes and virtual detectors. Virtual detectors are objects that do not correspond to a physical volume in the geometry but write entries in a ROOT TNtuple for each particle that passes through them. All materials used in shielding designs without ground are predefined in G4Beamline, and the soil material developed for later simulations is based on the median composition of world soils from Reference³. Cuts are performed in later simulations to exclude all particles except neutrons. For more complicated geometries, control structures were developed in G4Beamline to place shielding blocks based on parameters input by the user.

The first shielding geometry simulated in G4Beamline for this study consists of a wall of concrete blocks with configurable thickness, height, and width. Once the shielding blocks could be reliably placed without unphysical overlaps, a parameter to represent spacing between each block and its neighbors was introduced. The spacing parameter is used to represent the imperfect interfaces between the rough surfaces of shielding blocks stacked together. This shielding geometry is referred to as the spaced blocks geometry, and an example is given in Figure 1. A parameter was later introduced to place multiple x-y planes of shielding blocks along the z axis.

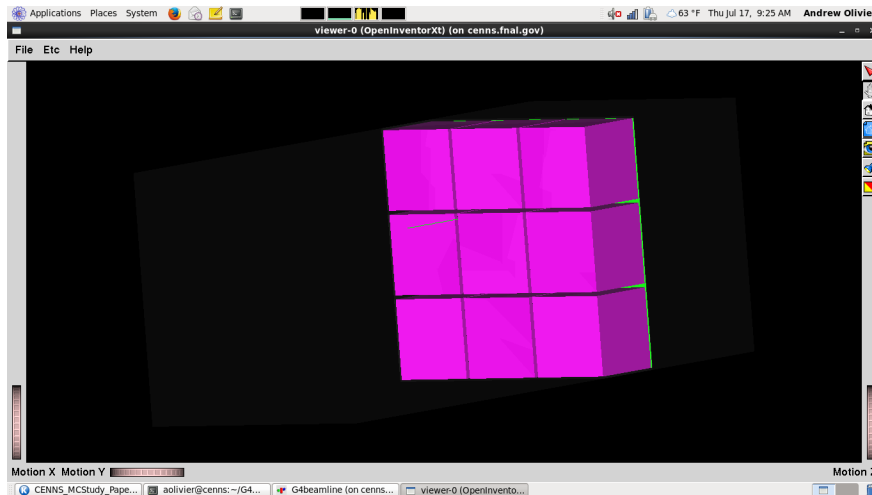


FIG. 1. Example of the spaced blocks geometry. The shielding blocks are magenta in this view. A particle from the beam specified by this simulation's configuration file, shown as a green line, travels through the shielding blocks along the z axis. The green rectangle behind the shielding blocks is a virtual detector.

The next geometry developed, the alternating blocks geometry, was designed using two layers of shielding blocks arranged so that the second layer covered holes in the first layer. The blocks in each shielding layer are separated by a spacing only in the y direction because it is impossible to build two layers of shielding that leave no gaps when separated in two directions. The capability to place multiple sets of layers of shielding blocks is maintained in this geometry. An example of the alternating shielding blocks geometry is included below in Figure 2.

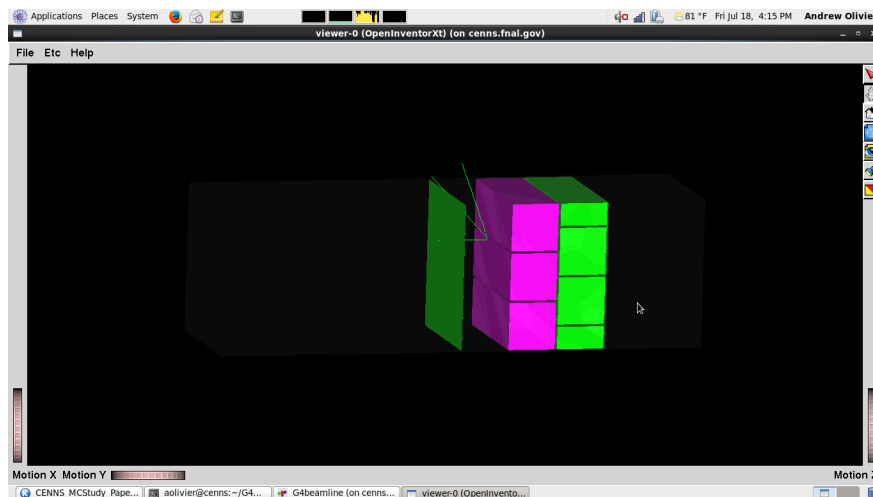


FIG. 2. Example of alternating blocks geometry. All alternating shielding blocks geometries have pairs of shielding blocks. In this image, the first layer is magenta, and the second layer, which blocks holes in the first layer, is green. Similar to the spaced blocks geometry, the alternating blocks geometry can place multiple pairs of shielding blocks based on a command line parameter.

Once the single plane shielding geometries had been used successfully in neutron shielding simulations, two more shielding block geometries that enclose a detector on three sides were developed. The spaced and alternating enclosed detector geometries consist of three planes of spaced blocks and alternating blocks geometries respectively. Two of the planes are rotated to be parallel to the beam to measure the effects of scattering off of these side shielding planes on the neutron spectrum observed by a detector placed behind the farthest downstream shielding blocks. An example of the enclosed detector geometry has been included in Figure 3, and an example of the alternating enclosed detector geometry is given in Figure 4.

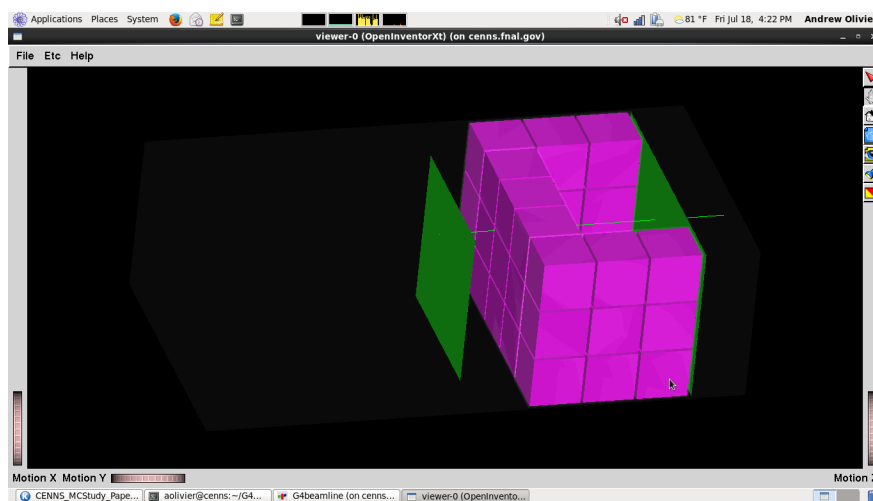


FIG. 3. Example of the enclosed detector shielding configuration. The magenta shielding blocks in this image enclose on three sides an area where a cube-shaped detector could be placed. The neutron spectra taken from this shielding geometry are typically recorded by the green virtual detector at the open end of the detector enclosure.

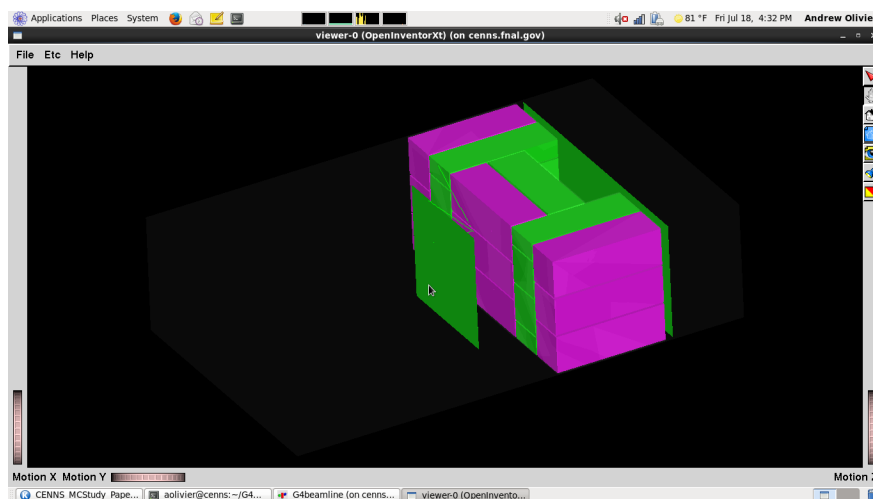


FIG. 4. Example of the alternating enclosed detector shielding geometry. The two types of layers of shielding blocks in this view of the alternating enclosed shielding configuration are colored magenta and green as in Figure 2. Neutron spectra for this geometry are read from the virtual detector behind the opening in the detector enclosure.

The next element added to the G4Beamline simulation of neutron shielding strategies for the CENNS experiment was a layer of soil placed below the detector and shielding blocks. Since no soil material was readily available in G4Beamline version 2.12, the median world soil content reported in Reference³ was implemented using the G4Beamline material command. A 10 m tall block of soil is simulated one shielding spacing below the bottom of each shielding geometry.

Concrete floor blocks were the last detail added to the CENNS neutron shielding study Monte Carlo. These blocks are separated by a distance equal to the shielding spacing of 5 mm used in later simulations from each other and the shielding geometries they are placed under. The floor blocks' dimensions are easily configurable from the command line when running G4Beamline. An example of the spaced blocks geometry with both 10 m of soil and concrete floor blocks is given below in Figure 5.

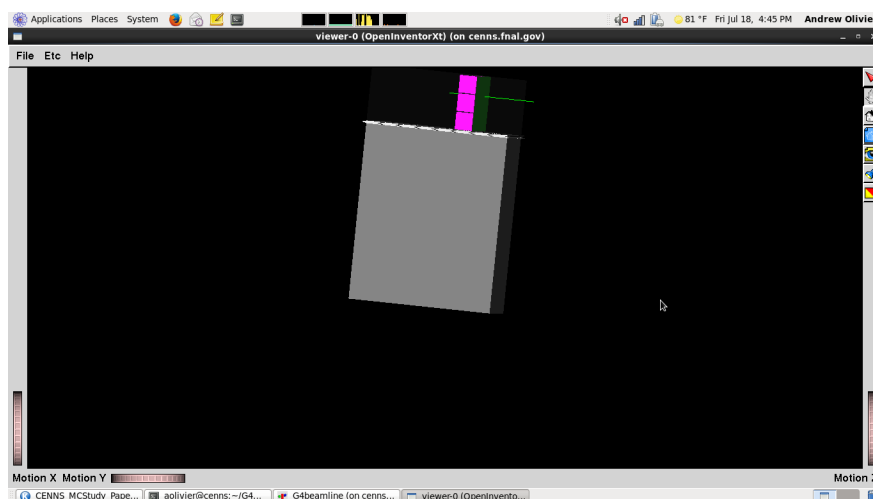


FIG. 5. Example of the spaced blocks shielding configuration with floor blocks and soil implemented. The ground block is the large grey box below the magenta shielding blocks. The soil material of which the ground is composed was constructed based on the median world soil content in Reference³. The concrete floor blocks are the white surface between the ground block and the lowest shielding blocks.

III. ANALYSIS

When a simulation is complete, G4Beamline can output a ROOT file containing an ntuple for each virtual detector with information about the events that passed through that detector. In later simulations, these ROOT files were collected in a directory structure with one directory for each shielding thickness and spacing included in the main directory and analyzed by a ROOT macro that produced histograms of the kinetic energies of the neutrons detected. Neutrons were selected to be included in ntuples in G4Beamline by setting the “require” parameter for each virtual detector to cut on PDG code. The histogramming macro included data from a G4Beamline simulation of the beam file with only a virtual detector near the origin for comparison with the other neutron spectra. The last set of histograms of kinetic energy were also normalized by the analysis macro so that their y axes represented the number of neutrons expected per m^2 per beam pulse of $4.5 \cdot 10^{12}$ POT. The value used to normalize the histograms was calculated as the integral of the neutron kinetic energy spectrum observed by the SciBath detector during the run described in Reference¹ in the range of energies the detector could accurately measure, 40 MeV to 200 MeV, divided by the integral of the neutron spectrum of the beam file over the same range.

IV. RESULTS

G4Beamline simulations of the proposed CENNS neutron shielding study produced histograms of the kinetic energy spectra expected for four shielding geometries at three different shielding block thicknesses. The results of the completed Monte Carlo study could be produced either with bins filled by the numbers of neutrons or normalized using Figure 14 in Reference¹ to represent the number of neutrons per m^2 per beam pulse expected in each energy bin. The number of neutrons histograms for the four geometries simulated for the CENNS neutron shielding study with floor blocks and soil implemented are included in Figures 6, 7, and 8. The normalized histograms for these geometries are included in Figures 9, 10, and 11.

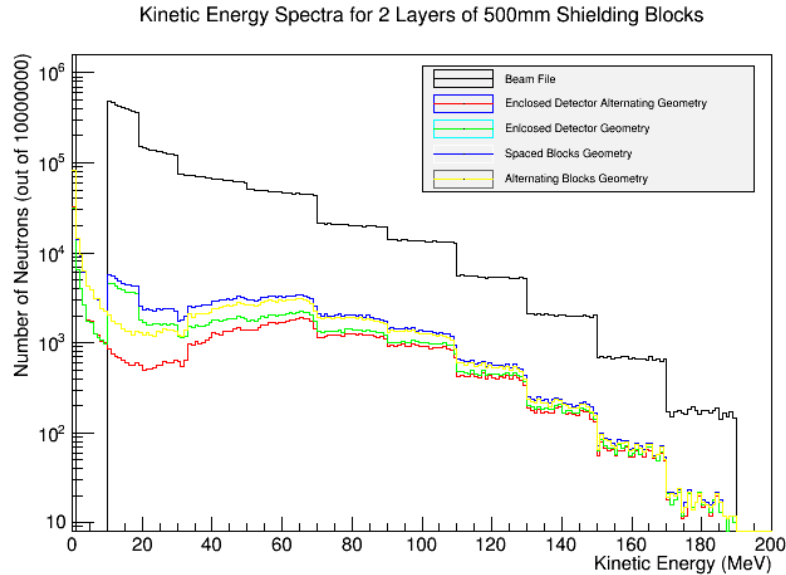


FIG. 6. Kinetic energy spectra for shielding geometries with 2 layers of 500 mm shielding blocks. This histogram includes both ground and concrete floor blocks in the simulated geometries. The alternating and enclosed detector alternating shielding strategies have the smallest bin contents in the 10 to 30 MeV kinetic energy range where nuclear recoils similar to neutrino interactions are likely to be detected in a CENNS experiment. At higher energies, the enclosed detector alternating geometry spectrum remains the lowest while all geometries’ histograms grow significantly more similar.

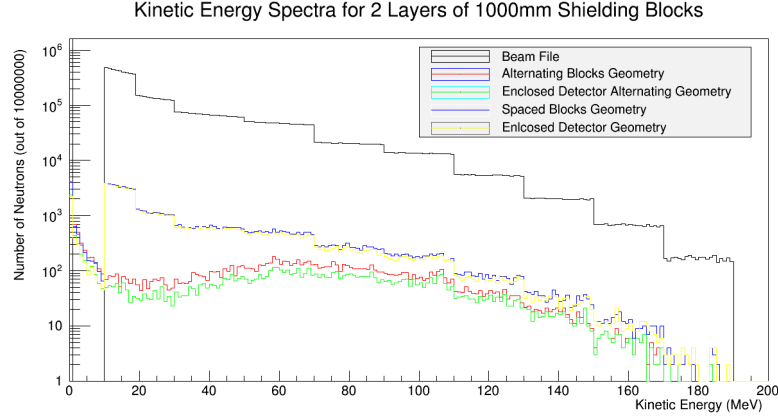


FIG. 7. Kinetic energy spectra for shielding geometries with 2 layers of 1 000 mm shielding blocks. This histogram includes floor blocks and soil in the results presented. The alternating and enclosed detector alternating shielding geometries have the lowest number of neutrons in the 10-30 MeV range. In this low kinetic energy range, the alternating geometries' neutron spectra are particularly well separated from the spaced block geometries. At higher kinetic energies, the spectra for all four geometries grow more similar with kinetic energy.

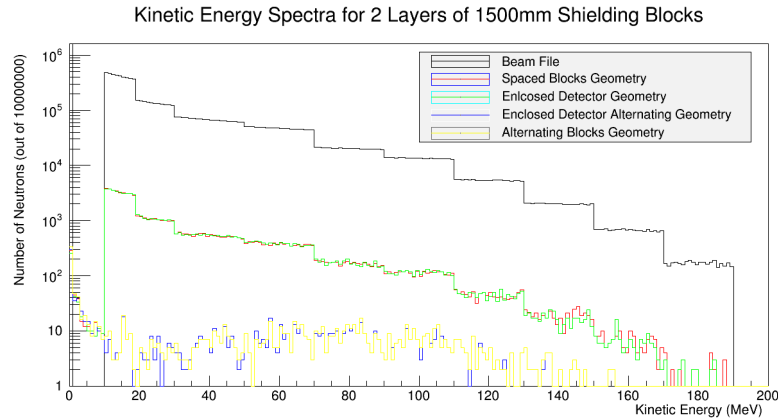


FIG. 8. Kinetic energy spectra for shielding geometries with 2 layers of 1 500 mm shielding blocks. This histogram includes both soil and concrete floor blocks as in the above figures. While the spectra for the spaced block geometries remain similar to their counterparts with thinner shielding blocks above, the alternating block strategies have bin values significantly lower than in previous histograms. The difference in shape between spaced and alternating geometries in the 10-30 MeV range remains a notable feature of this figure.

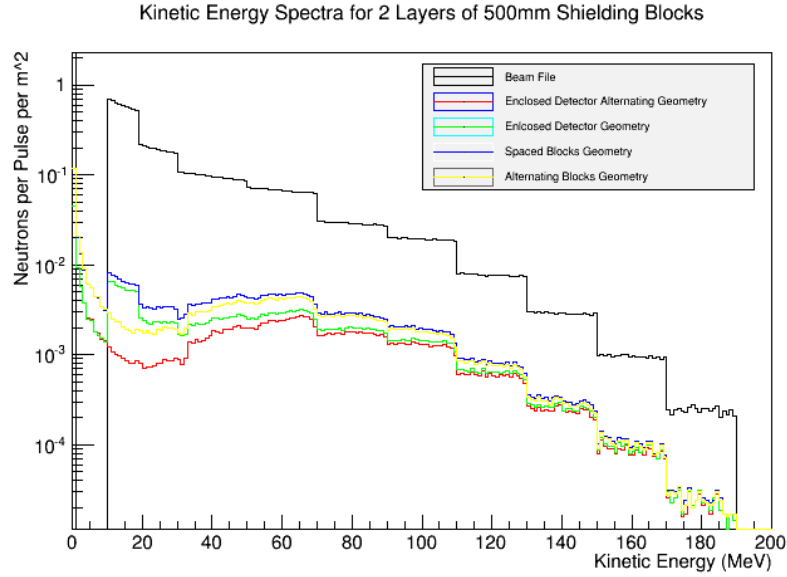


FIG. 9. Normalized kinetic energy spectra for shielding geometries with 2 layers of 500 mm shielding blocks. This histogram is identical to Figure 6 except for its y axis. The spectra in this figure have been normalized using information from Figure 14 in Reference¹ and the beam file used to run this simulation so that the y axis represents the number of neutrons/m²/(4.5*10¹² POT).

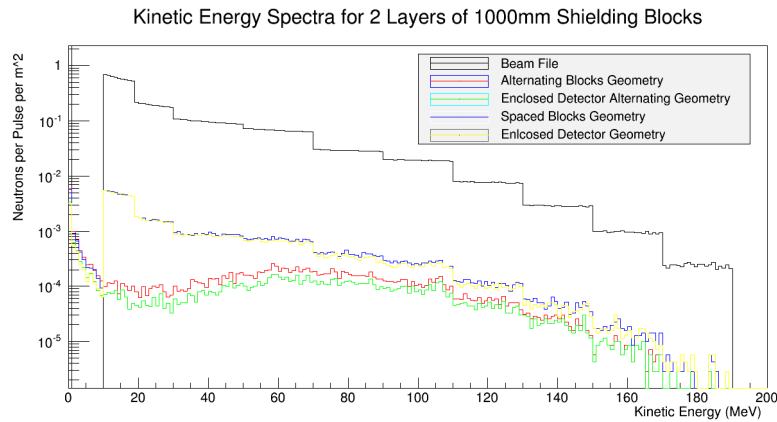


FIG. 10. Normalized kinetic energy spectra for shielding geometries with 2 layers of 1 000 mm shielding blocks. This histogram is identical to Figure 7 except for its y axis. The spectra in this figure have been normalized using information from Figure 14 in Reference¹ and the beam file used to run this simulation so that the y axis represents the number of neutrons/m²/(4.5*10¹² POT).

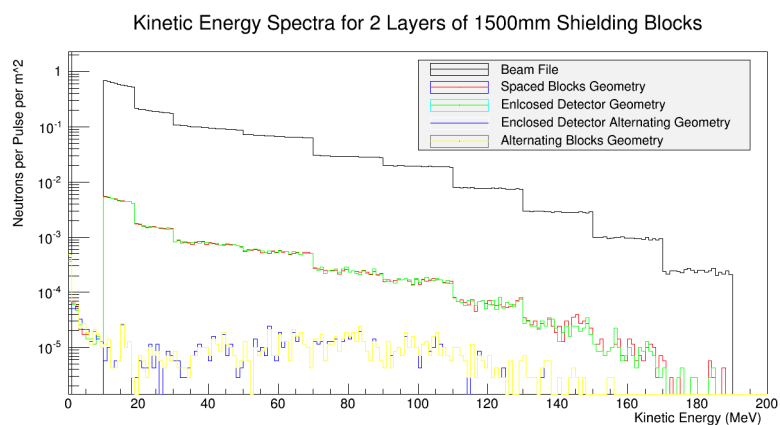


FIG. 11. Normalized kinetic energy spectra for shielding geometries with 2 layers of 1 500 mm shielding blocks. This histogram is identical to Figure 8 except for its y axis. The spectra in this figure have been normalized using information from Figure 14 in Reference¹ and the beam file used to run this simulation so that the y axis represents the number of neutrons/m²/(4.5*10¹² POT).

V. CONCLUSIONS AND DISCUSSION

According to the results of the CENNS neutron shielding Monte Carlo Simulation shown in Figures 9, 10, and 11, the enclosed detector alternating shielding blocks geometry is expected to be the most effective shielding strategy for stopping neutrons in the 10-30 MeV kinetic energy range. In addition, Figure 9 shows that only 1 m of concrete shielding blocks is expected to reduce the neutron spectrum at a potential detector in the enclosed detector alternating blocks geometry by almost three orders of magnitude, and at 3 m of shielding, the neutron flux is expected to decrease by almost five orders of magnitude. These results show that the enclosed detector alternating blocks shielding geometry is expected to be as effective at reducing neutron flux as the order of magnitude per meter of concrete estimated in Reference¹. Figure 12 below shows neutron flux reduction factors for the enclosed detector alternating blocks geometry.

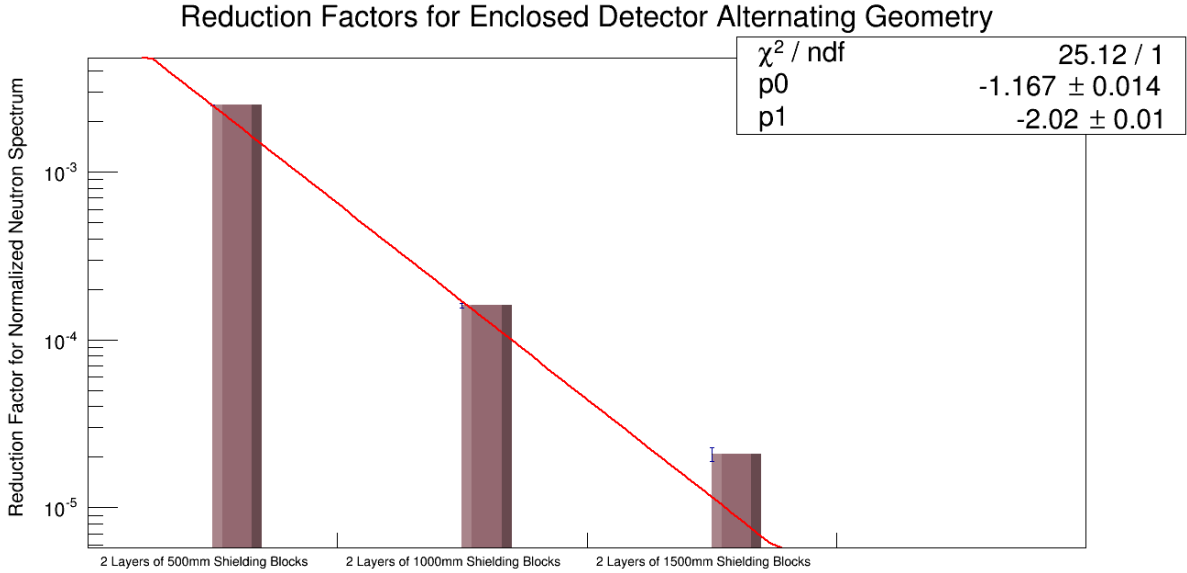


FIG. 12. Reduction factors for the enclosed detector alternating blocks geometry with various shielding block thicknesses. This figure shows the order of magnitude reductions for the enclosed detector alternating blocks geometry. The histogram was produced by the CENNS Neutron Shielding Monte Carlo analysis macro for the normalized histogram with the smallest integral in the 10-30 MeV range. The change in reduction factor per meter of concrete by about one order of magnitude is consistent with the results of a previous Monte Carlo study of neutron shielding for CENNS whose results are given in Reference¹. The fit to this histogram shown as a red line is of the form $10^{p_0 \cdot x + p_1}$, and it will be used to produce rough estimates of the neutron spectrum reduction factor measured experimentally. The large χ^2 is acceptable for this plot because it is only intended to produce order of magnitude results. The error bars included on each bar in this figure were calculated using an uncertainty of \sqrt{n} for the integrals of the beam file and the spectrum for each shielding configuration and propagating that error for the ratio of the two integrals.

Another interesting result of this study is the similarity in spectra for geometries with the same block placement strategy. In Figures 9, 10, and 11, the spectra for the alternating and enclosed detector alternating geometries as well as the enclosed and spaced blocks geometries become almost identical as shielding thickness increases. Thus, these histograms show that enclosing a detector in concrete shielding blocks on three sides only slightly decreases the neutron spectrum with smaller shielding blocks and may not make any significant difference in neutron flux when using more layers of shielding blocks.

Future work with this Monte Carlo simulation should begin with a study of the dependence of neutron spectra in various shielding strategies on the angular distribution of the neutrons' momenta. The effectiveness of the enclosed detector geometries in attenuating a neutron beam entering at an angle relative to the z axis is a study of particular interest in light of the reported neutron direction spectrum in Reference¹. In order to carry out studies with beams not parallel to the z axis, a box shaped virtual detector resembling

the SciBath detector should be added to the simulation to be used in place of the detectors placed at the downstream end of the shielding in this study. Scattering off of the surface of and within the detector should also be accounted for by constructing a G4beamline detector object out of a material with properties similar to the scintillator used in SciBath. Cosmic ray studies are also relevant to this experiment, so a concrete roof should be added above the detector in the simulation to understand the cosmogenic neutron flux to be expected. Current plans for CENNS neutron shielding measurements include placing SciBath and an array of neutron detectors discussed in Reference¹ inside a metal trailer within the shielding structure. The metal from the trailer as well the neutron detectors and other equipment necessary to operate SciBath may cause changes in the neutron spectrum inside the shielding geometry, so these elements should be added to the simulation for completeness.

VI. ACKNOWLEDGEMENTS

The author is grateful to J. Yoo for providing mentoring and support in developing objectives and implementation of Monte Carlo simulation. This work is supported by the Department of Energy Science Undergraduate Laboratory Internship program.

VII. REFERENCES

- ¹ S. Brice, R. Cooper, F. DeJongh, A. Empl, L. Garrison, et al., Phys.Rev. **D89**, 072004 (2014), 1311.5958.
- ² T. Roberts, Muons Inc (2012).
- ³ L. Wielopolski, Z. Song, I. Orion, A. L. Hanson, and G. Hendrey, Applied radiation and isotopes **62**, 97 (2005).